Article

Origin of Enantioselectivity in the Asymmetric Ru-Catalyzed Metathesis of Olefins

Chiara Costabile, and Luigi Cavallo

J. Am. Chem. Soc., **2004**, 126 (31), 9592-9600• DOI: 10.1021/ja0484303 • Publication Date (Web): 17 July 2004

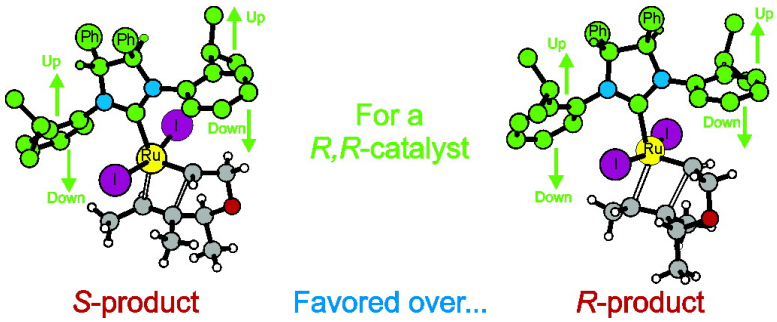

More About This Article

Additional resources and features associated with this article are available within the HTML version:

- Supporting Information
- Links to the 8 articles that cite this article, as of the time of this article download
- Access to high resolution figures
- Links to articles and content related to this article
- Copyright permission to reproduce figures and/or text from this article

View the Full Text HTML

J|A|C|S
ARTICLES
Published on Web 07/17/2004

Origin of Enantioselectivity in the Asymmetric Ru-Catalyzed Metathesis of Olefins

Chiara Costabile and Luigi Cavallo*

Contribution from the Dipartimento di Chimica, Università di Salerno, Via Salvador Allende, Baronissi (SA) I-80184, Italy

Received March 18, 2004; E-mail: lcavallo@unisa.it

Abstract: The mechanism of enantioselectivity in the asymmetric Ru-catalyzed metathesis of olefins is investigated with a theoretical approach. The models are based on the chiral N-heterocyclic (NHC)-based catalysts developed by Grubbs. Our analysis indicates that the origin of enantioselectivity in the ring-closing metathesis of achiral trienes is correlated to the chiral folding of the N-bonded aromatic groups, which is imposed by the Ph groups in positions 4 and 5 of the imidazole ring of the NHC ligand. This chiral folding of the catalyst imposes a chiral orientation around the Ru=C bond, which, in turn, selects between the two enantiofaces of the substrate. In the ring-closing transition state, the geometry in which additional groups on the forming ring are in pseudoequatorial positions is favored over transition states in which this additional group is in a pseudoaxial position. These combined effects rationalize the enantiomeric excesses experimentally obtained.

Introduction

Design of effective catalysts for asymmetric synthesis is a major challenge in modern chemistry. This achievement requires large amounts of intellectual, experimental, and economic investments. Catalyst development usually proceeds first through the discovery of an effective but nonenantioselective catalyst, followed by desymmetric evolution. Ru- and Mo-based catalysts active in the metathesis of olefins are following this route.[1−5]

It took only a few years for Ru-based catalysts to assume a prominent role not only in small-scale laboratory research chemistry, but also in large-scale industrial production chemistry,[6] and the last generation is based on (pre)catalysts with an N-heterocyclic (NHC) ligand (Chart 1, structure **1**).[7−9]

Several experimental studies shed light on the mechanisms that involve these catalysts,[10−21] and some molecular modeling studies subsequently provided a theoretical framework for the experimental findings.[22−31] These studies culminated in the mechanism of Scheme 1 as the most plausible.

Chart 1

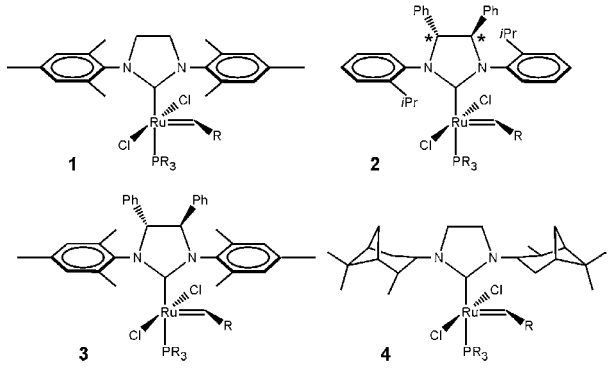

(1) Fürstner, A. *Angew. Chem., Int. Ed.* **2000**, *39*, 3012.
(2) Trnka, T. M.; Grubbs, R. H. *Acc. Chem. Res.* **2001**, *34*, 18.
(3) Hoveyda, A. H.; Schrock, R. R. *Chem.—Eur. J.* **2001**, *7*, 945.
(4) Hoveyda, A. H.; Schrock, R. R. *Compr. Asymmetric Catal., Suppl.* **2004**, *1*, 207.
(5) Grubbs, R. H. *Handbook of Olefin Metathesis*; Wiley-VCH: Weinheim, Germany, 2003.
(6) Rouhi, M. A. *Chem. Eng. News* **2002**, *80*, 29.
(7) Scholl, M.; Ding, S.; Lee, C. W.; Grubbs, R. H. *Org. Lett.* **1999**, *1*, 953.
(8) Huang, J.; Stevens, E. D.; Nolan, S. P.; Peterson, J. L. *J. Am. Chem. Soc.* **1999**, *121*, 2674.
(9) Weskamp, T.; Kohl, F. J.; Hieringer, W.; Gleich, D.; Herrmann, W. A. *Angew. Chem., Int. Ed.* **1999**, *38*, 2416.
(10) Dias, E. L.; Nguyen, S. T.; Grubbs, R. H. *J. Am. Chem. Soc.* **1997**, *119*, 3887.
(11) Hinderling, C.; Adlhart, C.; Baumann, H.; Chen, P. *Angew. Chem., Int. Ed.* **1998**, *37*, 2685.
(12) Adlhart, C.; Hinderling, C.; Baumann, H.; Chen, P. *J. Am. Chem. Soc.* **2000**, *122*, 8204.
(13) Adlhart, C.; Volland, M. A. O.; Hofmann, P.; Chen, P. *Helv. Chim. Acta* **2000**, *83*, 3306.
(14) Adlhart, C.; Chen, P. *Helv. Chim. Acta* **2000**, *83*, 2192.
(15) Sanford, M. S.; Ulman, M.; Grubbs, R. H. *J. Am. Chem. Soc.* **2001**, *123*, 749.
(16) Sanford, M. S.; Love, J. A.; Grubbs, R. H. *J. Am. Chem. Soc.* **2001**, *123*, 6543.
(17) Ulman, M.; Grubbs, R. H. *Organometallics* **1998**, *17*, 2484.
(18) Chatterjee, A. K.; Choi, T.-L.; Sanders, D. P.; Grubbs, R. H. *J. Am. Chem. Soc.* **2003**, *125*, 11360.
(19) Bassetti, M.; Centola, F.; Semeril, D.; Bruneau, C.; Dixneuf, P. H. *Organometallics* **2003**, *22*, 4459.
(20) Love, J. A.; Sanford, M. S.; Day, M. W.; Grubbs, R. H. *J. Am. Chem. Soc.* **2003**, *125*, 10103.
(21) Trnka, T. M.; Morgan, J. P.; Sanford, M. S.; Wilhelm, T. E.; Scholl, M.; Choi, T.-L.; Ding, S.; Day, M. W.; Grubbs, R. H. *J. Am. Chem. Soc.* **2003**, *125*, 2546.
(22) Aagaard, O. M.; Meier, R. J.; Buda, F. *J. Am. Chem. Soc.* **1998**, *120*, 7174.
(23) Bernardi, F.; Bottoni, A.; Miscione, G. P. *Organometallics* **2000**, *19*, 5529.
(24) Meier, R. J.; Aagaard, O. M.; Buda, F. *J. Mol. Catal. A* **2000**, *160*, 189.
(25) Volland, M. A.; Hansen, S. M.; Hofmann, P. In *Chemistry at the Beginning of the Third Millennium*; Fabbrizzi, L., Poggi, A., Eds.; Springer: Berlin, 2000; p 23.
(26) Vyboishchikov, S. F.; Bühl, M.; Thiel, W. *Chem.—Eur. J.* **2002**, *8*, 3962.
(27) Cavallo, L. *J. Am. Chem. Soc.* **2002**, *124*, 8965.
(28) Adlhart, C.; Chen, P. *Angew. Chem., Int. Ed.* **2002**, *41*, 4484.
(29) Bernardi, F.; Bottoni, A.; Miscione, G. P. *Organometallics* **2003**, *22*, 940.
(30) Adlhart, C.; Chen, P. *J. Am. Chem. Soc.* **2004**, *126*, 3496.
(31) Suresh, C. H.; Koga, N. *Organometallics* **2004**, *23*, 76.

10.1021/ja0484303 CCC: $27.50

Scheme 1

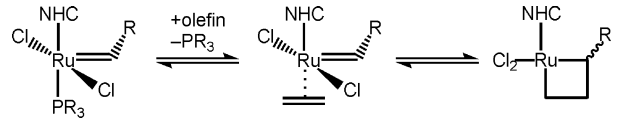

Chart 2

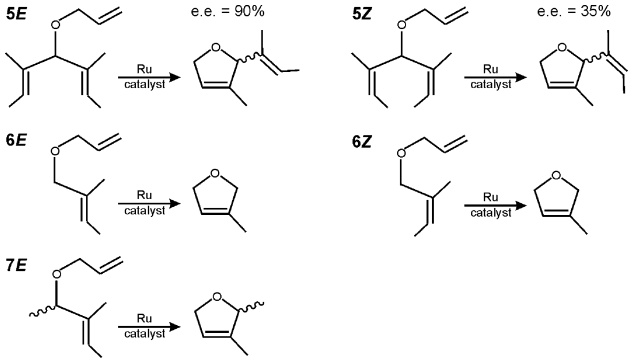

Scheme 2

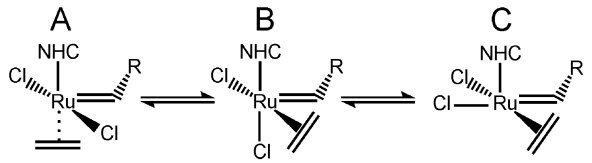

Recently, the first reports of asymmetric olefin metathesis appeared in the literature.[32−34] For the Ru catalysts this result was obtained through desymmetrization of the NHC ligand (Chart 1, structure **2**).[33] Two structural modifications are required to transform the parent NHC ligand of **1** into that of **2**. First, chirality is introduced to the NHC ring by placement of two phenyl groups in positions 4 and 5 of the imidazole ring. This generates the two chiral C atoms marked by asterisks in Chart 1. Second, since the so-generated stereocenters are remote from the metal, Grubbs and co-workers replaced the mesityl substituents of **1** with mono-*ortho*-substituted aryl groups. They argued this substitution should lead to a more effective transfer of stereochemical information from the ligand nearer to the metal center. The rationally designed structure **2** is effective in the asymmetric ring-closing metathesis of achiral substrates (Chart 2, structure **5**), and higher enantiomeric excesses (ee) are obtained for (*E*)-olefins such as **5*E*** than for the corresponding (*Z*)-isomer **5*Z***.[33] Of course, understanding the mechanism of enantioselectivity with these catalysts is likely to have practical consequences.

In this respect, Grubbs and co-workers raised the question of whether the geometry of the crucial intermediate indeed corresponds to the most often proposed isomer with the olefin coordinated *trans* to the NHC ligand (**A** in Scheme 2). In fact, alternative isomers with the olefin coordinated *cis* to the NHC ligand (**B** and **C** in Scheme 2) are characterized by greater proximity between the olefin and the chiral centers.[33] This point is based on the well-accepted idea that effective asymmetric catalysis requires proximity between the point of chirality and the reacting atoms.[35]

Since asymmetric olefin metathesis is at the first stages of development, and the origin of enantioselectivity is still unclear, we believe that a molecular modeling study could be extremely useful. If practical, it will provide valuable insights for further development of catalysts, resulting in higher enantiomeric excesses. Stereoselective polymerization of 1-olefins is a clear example of synergic experimental and theoretical development of new catalysts.[36] Furthermore, understanding the mechanisms that rule the behavior of a given class of catalysts is also useful to devise new applications for the already discovered catalysts.[37]

Here we present a quantum mechanics/molecular mechanics (QM/MM) study on the origin of enantioselectivity with the catalyst derived from **2**. Instead of directly calculating the enantioselectivity in the ring-closing metathesis of **5*E*** with the catalysts derived from **2**, we preferred a different approach. We believe that a simple rationalization of experimental behavior is not particularly useful to the chemical community if it is not accompanied by a detailed explanation and rationalization that could permit a deeper understanding of these systems. For this reason, we first report on which of the isomers **A**−**C** is the most likely intermediate in the ring-closing metathesis. Subsequently, we investigate whether one of the two enantiofaces of the second C═C double bond of the substrate preferentially coordinates/reacts in the presence of a chiral catalyst. We briefly recall that coordination of a prochiral C═C double bond to a metal atom is chiral (see the Models and Nomenclature sections). Finally, after these points have been clarified, we report on the connection between the chirality of the catalyst and the enantioselectivity of the ring-closing metathesis step. This kind of analysis should allow a detailed understanding of the mechanism and of the flow of information that starts from the chirality of the ligand and results in effective asymmetric catalysis.

The results will be presented as follows: (i) using the model and simple (*E*)-olefin **6*E*** of Chart 2, we discuss the relative stability of isomers **A**−**C**; (ii) using the same model olefin **6*E***, we discuss olefin enantioface selectivity in the C−C bond (metallacycle) formation; (iii) using the chiral model (*E*)-olefin **7*E***, we discuss the relationship between enantioface selectivity and configuration of the products. The simpler olefin **6*E*** in points i and ii allows for an easier rationalization of the results. The configuration of the catalyst, determined by the configuration of the chiral C atoms in positions 4 and 5 of the imidazole ring, is always *R*,*R* (see Figure 1), which experimentally leads to the (*S*)-enantiomer as the major product.[33]

To validate the mechanism we developed, we tested it on the enantioselectivity of (i) the model (*Z*)-olefin **6*Z*** with a model of the catalyst derived from **2** and (ii) olefin **6*E*** with models of catalysts derived from **3** and **4** of Chart 1. In both these cases, low ee values were obtained experimentally.[33] Finally, a short paragraph is also dedicated to the role of the halogen atoms on the enantioselective performances of **2**. Experimentally, the heavier the halogen, the greater the ee obtained in the desymmetrization of achiral substrates such as **5**.[33]

(32) Alexander, J. B.; La, D. S.; Cefalo, D. R.; Hoveyda, A. H.; Schrock, R. R. *J. Am. Chem. Soc.* **1998**, *120*, 4041.
(33) Seiders, T. J.; Ward, D. W.; Grubbs, R. H. *Org. Lett.* **2001**, *3*, 3225.
(34) Van Veldhuizen, J. J.; Garber, S. B.; Kingsbury, J. S.; Hoveyda, A. H. *J. Am. Chem. Soc.* **2002**, *124*, 4954.
(35) Lipkowitz, K. B.; D'Hue, C. A.; Sakamoto, T.; Stack, J. N. *J. Am. Chem. Soc.* **2002**, *124*, 14255.
(36) Resconi, L.; Cavallo, L.; Fait, A.; Piemontesi, F. *Chem. Rev.* **2000**, *100*, 1253.
(37) Guerra, G.; Longo, P.; Corradini, P.; Cavallo, L. *J. Am. Chem. Soc.* **1999**, *121*, 8651.

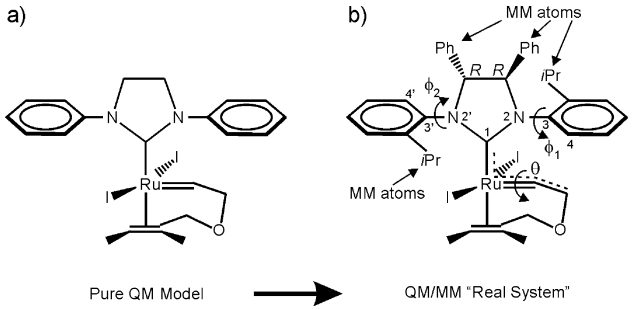

Figure 1. Representation of the partitioning of the systems into QM and MM regions, and definition of the dihedral angles ϕ_1, ϕ_2, and θ. The configuration (*R*,*R*) of the chiral C atoms in positions 4 and 5 of the imidazole ring is also indicated.

Scheme 3

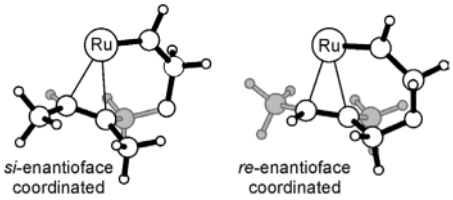

Models and Computational Details

Models. The models we considered are derived from the (pre)-catalysts **2**−**4**, in which the phosphine *trans* to the NHC ligand has been removed, and the ═CHPh group bonded to Ru has been replaced with the ═$CHCH_2OCHRC(CH_3)$═$CH(CH_3)$ group, with R = H or CH_3. For the case of the catalyst derived from **2** and R = H, the corresponding system is illustrated in Figure 1b. Moreover, we replaced the original Cl atoms of **2**−**4** with iodine atoms, since higher enantiomeric excesses are obtained experimentally for systems with I as the halide.[33]

Coordination of a prochiral olefin to a metal atom, such as the substrates of Chart 2, gives rise to nonsuperimposable coordinations.[38] As an example, the two chiral geometries that originate from coordination of the second C═C double bond of **6*E*** in the intermediate that immediately precedes the ring-closing step are illustrated in Scheme 3.

To distinguish between coordinations of the two enantiofaces, we prefer the nomenclature *re*/*si*, defined for specifying heterotopic half-spaces,[38] instead of the nomenclature *R*/*S*, defined for double or triple bonds π-bonded to a metal atom.[39,40] To avoid confusion, we will reserve the symbols *R*/*S* to define the configuration of the chiral sp^3 C atoms in both reactants and products.

To facilitate the geometrical characterization of the structures, we define the dihedral angles ϕ_1 and ϕ_2 (see Figure 1), which are the dihedral angles C1−N2−C3−C4 and C1−N2′−C3′−C4′. Values of ϕ_1 and $\phi_2 = |90°|$ correspond to the plane of the N-bonded aromatic rings being orthogonal to the N2−C1−N2′ plane. Finally, we also define the dihedral angle θ, which is the dihedral angle C1−Ru═C−CH_2 (see Figure 1).

Computational Details. The Amsterdam density functional (ADF) program was used to obtain all the results discussed herein.[41,42] The electronic configuration of the molecular systems was described by a triple-ζ STO basis set on ruthenium for 4s, 4p, 4d, 5s, and 5p (ADF basis set IV).[41] Double-ζ STO basis sets were used for iodine (5s, 5p), oxygen, nitrogen, and carbon (2s, 2p), and hydrogen (1s), augmented with single 5d, 3d, 3d, 3d, and 2p functions, respectively (ADF basis set III).[41] The inner shells on ruthenium (including 3d), iodine (including 4d), and oxygen, nitrogen, and carbon (1s) were treated within the frozen core approximation. Energies and geometries were evaluated using the local exchange-correlation potential by Vosko et al.,[43] augmented in a self-consistent manner with Becke's[44] exchange gradient correction and Perdew's[45,46] correlation gradient correction. Relativistic effects were included self-consistently with the zeroth-order relativistic approximation (ZORA).[47−49] To evaluate solvent effects, test calculations of the solvation energies were obtained from a single-point full QM calculation using the conductor-like screening model (COSMO)[50,51] and optimized geometries from QM/MM calculations. A dielectric constant of 7.58 was used to represent tetrahydrofuran as the solvent. The radii used for the atoms (Å) were as follows: H, 1.29; C, 2.00; N, 1.83; O, 1.71; I, 2.31; Ru, 2.30.

The ADF program was modified by one of us[52−54] to include standard molecular mechanics force fields in such a way that the QM and MM parts are coupled self-consistently.[54,55] The simple model QM systems and the full QM/MM and QM systems are displayed in Figure 1. The partitioning of the systems into QM and MM parts only involves the NHC ligand. Specifically, the Ph groups in the 4 and 5 positions of the imidazolyl ring, and the *i*-Pr groups of the N-bonded aromatic rings, are treated as MM atoms.

As for the connection between the QM and MM parts, this occurs by means of the so-called "capping" dummy atoms, which are replaced in the real system by the corresponding "linking" atom.[54,55] H atoms were used as capping atoms for all the C(aromatic)−C(sp^3) linking bonds. In the QM/MM optimizations the ratio between the distances of the C−C bonds crossing the QM/MM border and the corresponding optimized C−H distance was fixed to 1.40. A more detailed description of the coupling scheme, as well as further comments on the methodology, can be found in previous papers.[52,54] The AMBER95 force field[56] was used for the MM potentials, except for Ru and I, which were treated with the UFF force field.[57] To eliminate spurious stabilizations from the long-range attractive part of the Lennard-Jones potential,[52,58] we used an exponential expression fitted to the repulsive part of the Lennard-Jones potential.[52,59−61]

The minima were localized by full optimization of the starting structures. Convergence criteria in the geometry optimizations were set to 1×10^{-3} au on the maximum Cartesian gradient. Transition states were approached through a linear transit procedure which started from the coordination intermediates. The distance between the two C atoms which would form the new C−C bond was assumed as the reaction coordinate. At each point, the C−C distance assumed as the reaction

(38) Hanson, K. R. *J. Am. Chem. Soc.* **1966**, *88*, 2731.
(39) Cahn, R. S.; Ingold, C.; Prelog, V. *Angew. Chem., Int. Ed. Engl.* **1966**, *5*, 385.
(40) Corradini, P.; Paiaro, G.; Panunzi, A. *J. Polym. Sci., Part C* **1967**, *16*, 2906.
(41) *ADF 2000, Users Manual*; Vrije Universiteit: Amsterdam, The Netherlands, 2000.
(42) te Velde, G.; Bickelhaupt, F. M.; Baerends, E. J.; Fonseca Guerra, C.; Van Gisbergen, S. J. A.; Snijders, J. G.; Ziegler, T. *J. Comput. Chem.* **2001**, *22*, 931.
(43) Vosko, S. H.; Wilk, L.; Nusair, M. *Can. J. Phys.* **1980**, *58*, 1200.
(44) Becke, A. *Phys. Rev. A* **1988**, *38*, 3098.
(45) Perdew, J. P. *Phys. Rev. B* **1986**, *33*, 8822.
(46) Perdew, J. P. *Phys. Rev. B* **1986**, *34*, 7406.
(47) van Lenthe, E.; Baerends, E. J.; Snijders, J. G. *J. Chem. Phys.* **1993**, *99*, 4597.
(48) van Lenthe, E.; Baerends, E. J.; Snijders, J. G. *J. Chem. Phys.* **1994**, *101*, 9783.
(49) van Lenthe, E.; Ehlers, A. E.; Baerends, E. J. *J. Chem. Phys.* **1999**, *110*, 8943.
(50) Klamt, A.; Schüürmann, G. *J. Chem. Soc., Perkin Trans. 2* **1993**, 799.
(51) Pye, C. C.; Ziegler, T. *Theor. Chem. Acc.* **1999**, *101*, 396.
(52) Cavallo, L.; Woo, T. K.; Ziegler, T. *Can. J. Chem.* **1998**, *76*, 1457.
(53) Deng, L.; Woo, T. K.; Cavallo, L.; Margl, P. M.; Ziegler, T. *J. Am. Chem. Soc.* **1997**, *119*, 6177.
(54) Woo, T. K.; Cavallo, L.; Ziegler, T. *Theor. Chem. Acc.* **1998**, *100*, 307.
(55) Maseras, F.; Morokuma, K. *J. Comput. Chem.* **1995**, *16*, 1170.
(56) Cornell, W. D.; Cieplak, P.; Bayly, C. I.; Gould, I. R.; Merz, K. M. J.; Ferguson, D. M.; Spellmeyer, D. C.; Fox, T.; Caldwell, J. W.; Kolmann, P. A. *J. Am. Chem. Soc.* **1995**, *117*, 5179.
(57) Rappé, A. K.; Casewit, C. J.; Colwell, K. S.; Goddard, W. A., III; Shiff, W. M. *J. Am. Chem. Soc.* **1992**, *114*, 10024.
(58) Sauers, R. R. *J. Chem. Educ.* **1996**, *73*, 1996.
(59) Lee, K. J.; Brown, T. L. *Inorg. Chem.* **1992**, *31*, 289.
(60) Woo, T. K.; Ziegler, T. *Inorg. Chem.* **1994**, *33*, 1857.
(61) Guerra, G.; Cavallo, L.; Corradini, P.; Longo, P.; Resconi, L. *J. Am. Chem. Soc.* **1997**, *119*, 4394.

coordinate was kept fixed while all the other degrees of freedom were fully optimized. Full transition-state searches were started from the structures corresponding to the maximum of the energy along the linear transit paths.

Results

Nomenclature. Structures discussed hereafter will be labeled, for example, as **2B**‡-**6*E*-*re*-*syn***, with the following meaning: (i) The first label, **2A**, **2B**, or **2C**, indicates which of the three isomers of Scheme 2 is considered for the systems derived from (pre)catalyst **2**. If the first label is followed by a superscript "‡", the structure is a transition state. (ii) The second label, such as **6*E*** or **7*Z***, indicates which substrate of Chart 2 is considered. (iii) The third label, ***re*** or ***si***, indicates which enantioface of the double bond of the substrate is coordinated to the metal. (iv) The fourth label, ***syn*** or ***anti***, holds only for structures derived from isomer **B**, and indicates the relative orientation of the two CH_3 groups of substrates such as **6*E*** with respect to the NHC ligand. Thus, **2B**‡-**6*E*-*re*-*syn*** indicates the transition state for the ring-closing metathesis of **6*E*** derived from isomer **B** of the catalyst derived from **2**. The coordinated enantioface of **6*E*** is *re*, and *syn* is the orientation of the two CH_3 groups of **6*E*** relative to the NHC ligand.

Stability of Isomers A−C. In this section we report on the relative stability and some geometric features of isomers **A**−**C** in the case of the model substrate **6*E*** with the catalyst derived from **2**. The structures we discuss, illustrated in Figure 2, correspond to the coordination intermediates that precede the transition states for the ring-closing metathesis of the model substrate **6*E***.

The two **A** structures we located, **2A-6*E*-*si*** and **2A-6*E*-*re***, correspond to coordination of the two enantiofaces of **6*E*** to the Ru atom. These structures are substantially isoenergetic, since **2A-6*E*-*re*** is only 1 kJ/mol higher in energy than **2A-6*E*-*si***. The dihedral angle θ of Figure 1 assumes a value close to 180° (see Table 1). In both structures it is the small H(carbene) atom that points toward the NHC ligand. This reduces steric interactions between the substrate and the NHC ligand. This finding is in agreement with the crystal structure of $(PCy_3)(t\text{BuO})_2$-Ru=CHPh, in which the =CHPh group is almost perpendicular to the O−Ru−O plane, with the H(carbene) atom pointing toward the Ru atom.[62] Finally, due to the overall C_2 symmetry of the catalyst in structures **A**, an exchange of the coordination position of the C(carbene) from right to left in structures **2A-6*E*-*si*** and **2A-6*E*-*re*** would lead to identical structures **2A-6*E*-*si*** and **2A-6*E*-*re*** with, of course, identical energies. This symmetry consideration holds for all the structures with the substrate coordinated *trans* to the NHC ligand.

All the **B** structures we calculated are more than 20 kJ/mol higher in energy than **2A-6*E*-*re*** (see Table 1). They are characterized by strong deformations which are caused by the bulkiness of the substrate. Structures **2B-6*E*-*si*-*syn*** and **2B-6*E*-*re*-*syn*** are destabilized by steric interactions between the N-bonded aromatic rings of the NHC ligand and the *syn*-oriented CH_3 groups of **6*E***. This is suggested by the short distances reported in Figure 2. Instead, structures **2B-6*E*-*si*-*anti*** and **2B-6*E*-*re*-*anti*** are destabilized mainly by steric interactions of the CH_2 group close to the coordinated C=C double bond.

(62) Sanford, M. S.; Henling, L. M.; Day, M. W.; Grubbs, R. H. *Angew. Chem., Int. Ed.* **2000**, *39*, 3451.

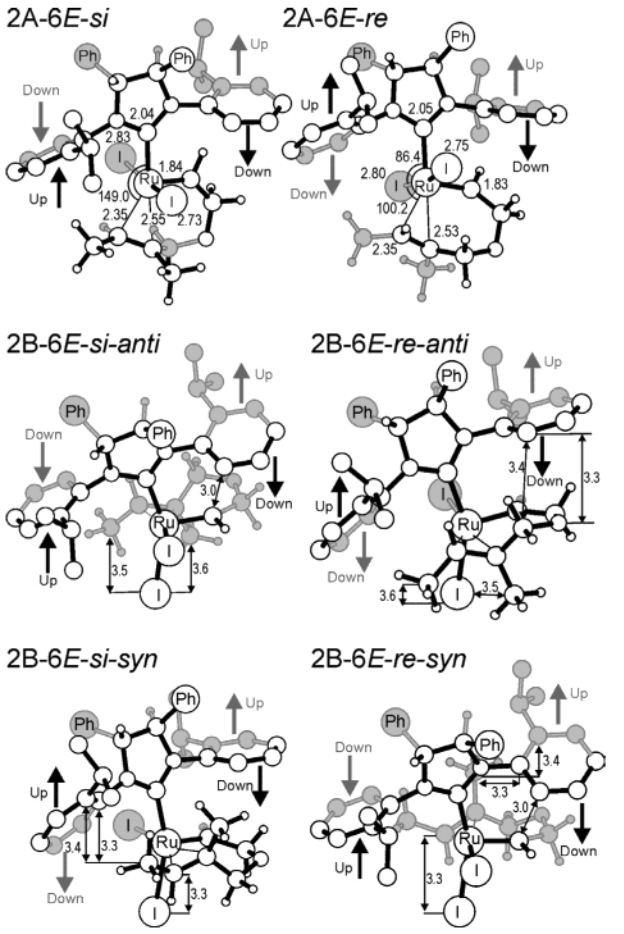

Figure 2. Geometries of the coordination intermediates corresponding to coordination of **6*E*** to the catalyst derived from **2**. Atoms of the system which are below the mean plane defined by the Ru=C bond and the NHC ring are colored in gray. For simplicity, the Ph groups in positions 4 and 5 of the NHC ring are represented as single large spheres. Distances are in angstroms, and angles are in degrees.

Considering the high energy of **B** isomers compared with **A** isomers, we believe the former contribute negligibly to olefin metathesis, and will not be discussed further. This conclusion is also based on the low barrier for metallacycle formation starting from **A** isomers (∼5−10 kJ/mol), and on recent and detailed theoretical studies which show that the preferential reaction path starts from isomer **A**.[26,30]

Finally, we were unable to locate geometries corresponding to isomer **C** for coordination of **6*E*** to the model of catalyst derived from **2**. Most of the attempts converged into one of the **B** isomers, while in the other cases they converged into one of the **A** isomers. We believe that our inability to locate the **C** isomer is due to the steric bulkiness of the NHC ligand, which pushes the halide atom *trans* to the Ru=C(carbene) bond toward the empty coordination position *trans* to the NHC ligand. This conclusion is also supported by similar results recently obtained by Adlhart and Chen for very closely related systems.[30]

From a geometrical standpoint, in the low-energy **A** structures the steric pressure of the Ph groups in positions 4 and 5 of the NHC ligand imposes a systematic chiral twisting of the N-bonded aromatic rings. To reduce steric interactions, both these rings rotate by roughly 15° from a perfect orthogonal orientation relative to the N−C−N plane of the NHC ring. The angles ϕ_1 and ϕ_2 (see Figure 1) deviate from −90° to assume

Table 1. Energies and Relevant Geometric Parameters of the Species Discussed[a]

system	*E* (kJ/mol)	θ (deg)	ϕ_1 (deg)	ϕ_2 (deg)
2A-6*E*-*si*	0	−176.4	−72.7	−72.9
2A-6*E*-*re*	1	141.8	−72.8	−73.5
2B-6*E*-*si*-*anti*	44	−97.1	−73.4	−82.3
2B-6*E*-*si*-*syn*	34	117.6	−64.5	−50.3
2B-6*E*-*re*-*syn*	63	−107.0	−63.7	−78.4
2B-6*E*-*re*-*anti*	28	98.8	−77.6	−65.7
2A‡-6*E*-*si*	0	−98.5	−73.8	−66.1
2A‡-6*E*-*re*	6	99.1	−65.4	−63.7
2A‡-6*E*-*si*-S_{eq}	0 (0)	−96.4	−72.9	−67.4
2A‡-6*E*-*re*-R_{eq}	10 (6)	97.6	−63.4	−66.0
2A‡-6*E*-*si*-R_{ax}	28 (29)	−98.6	−71.0	−68.7
2A‡-7*Z*-*si*	0	−96.2	−70.8	−63.3
2A‡-7*Z*-*re*	2	100.2	−68.2	−63.7
3A‡-6*E*-*si*	3	−97.4	−98.1	−96.7
3A‡-6*E*-*re*	0	96.5	−86.8	−95.1
4A‡-6*E*-*si*	1	−98.3	[b]	[b]
4A‡-6*E*-*re*	0	98.2	[b]	[b]

[a] The energy values in parentheses for entries **2A‡-6*E*-*si*-S_{eq}**, **2A‡-6*E*-*re*-R_{eq}**, and **2A‡-6*E*-*si*-R_{ax}** include solvent effects calculated as described in the Computational Details section. [b] The ϕ_1 and ϕ_2 angles are not defined for the systems derived from (pre)catalyst **4**.

values close to −75°. Similar values of ϕ_1 and ϕ_2 (−76° and −77°) are observed in the X-ray structure of a closely analogous complex.[33] Thus, the Ph groups desymmetrize the ligand, forcing the nearby side of the N-bonded aromatic rings (the one without the *i*-Pr group) to be bent down toward the equatorial coordination plane, which is the plane with the halide atoms and the Ru=carbene bond. Conversely, the other side of the ring (the one with the *i*-Pr group) is bent up, i.e., is pushed away from the equatorial plane. This chiral twisting of the N-bonded aromatic rings is a systematic feature of all the structures based on **2** that we calculated, whether they are coordination intermediates or transition states. We will demonstrate that this chiral twisting is at the origin of the enantioselectivity shown by these catalysts.

Concluding this part, our results indicate that coordination of the second C=C double bond of the substrate only selects between different isomers (**A** favored relative to **B** and **C**). However, at this point there is no influence of the chirality of the ligand because there is no enantioface selectivity, since **2A-6*E*-*si*** is only marginally favored relative to **2A-6*E*-*re***.

Olefin Enantioface Selectivity. In this section we report on the relative stability of the two transition states that can be reached from the low-energy coordination intermediates **2A-6*E*-*si*** and **2A-6*E*-*re***.

Starting from **2A-6*E*-*si*** and **2A-6*E*-*re***, we located the transition states **2A‡-6*E*-*si*** and **2A‡-6*E*-*re*** for ring-closing (and metallacycle formation) illustrated in Figure 3. Formation of the new C−C bond imposes a rotation around θ from roughly 180° to ca. −90° and +90° in **2A‡-6*E*-*si*** and **2A‡-6*E*-*re***, respectively (see Table 1). The sign assumed by the θ angle in the transition state is determined by the chirality of coordination of the substrate. Specifically, the *re* (*si*) enantioface imposes a positive (negative) value to θ. In both transition states these values of θ place the forming five-membered rings on one side of the forming metallacycle ring. This reduces steric interactions with other atoms and allows the forming five-membered ring

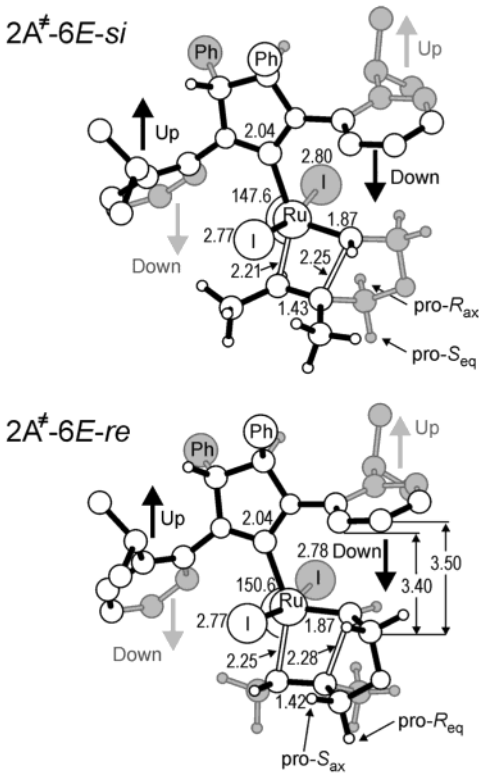

Figure 3. Transition states **2A‡-6*E*-*si*** and **2A‡-6*E*-*re***, corresponding to ring-closing metathesis of **6*E*** with the catalyst derived from **2**. Atoms of the system which are below the mean plane defined by the Ru=C bond and the NHC ring are shaded gray. For simplicity, the Ph groups in positions 4 and 5 of the NHC ring are represented as single large spheres. Distances are in angstroms, and angles are in degrees.

to assume a relaxed pseudoenvelope geometry with the O atom at the apex of the envelope.[63,64]

Although the two transition states of Figure 3 may seem rather similar, they have a substantial geometric difference. In the case of the *si* enantioface the forming five-memberd ring is close to the bent-up side of the nearby N-bonded aromatic group, while in the case of the *re* enantioface the forming ring is close to the bent-down part of the same N-bonded aromatic group. For **2A‡-6*E*-*re*** this results in steric interactions between the substrate and the bent-down side of the proximal aromatic group, as indicated by the short distances reported in Figure 3. In **2A‡-6*E*-*si*** these interactions are less relevant because the small H(carbene) atom is close to the bent-down side of the proximal aromatic group.

The different steric interactions in the two transition states result in a preference for the less strained **2A‡-6*E*-*si*** geometry, which is 6 kJ/mol lower in energy than **2A‡-6*E*-*re***. Thus, for an (*R*,*R*)-complex, transition states with $\theta \approx -90°$ are favored over those with $\theta \approx +90°$. Considering the previous discussion, this implies olefin enantioface selectivity, since values of $\theta \approx -90°$ and +90° impose reaction of the *si* and *re* enantiofaces, respectively. In this respect, the chiral folding of the catalyst forces a chiral orientation on the θ angle. This chiral orientation, in turn, selects between the two prochiral enantiofaces of the olefin. This mechanism of selectivity is rather similar to that operative in the stereospecific polymerization of olefins with

(63) Kilpatrick, J. E.; Pitzer, K. S.; Spitzer, R. *J. Am. Chem. Soc.* **1947**, *69*, 2483.
(64) Pitzer, K. S.; Donath, W. E. *J. Am. Chem. Soc.* **1959**, *81*, 3213.

group 4 metals,[36,65,66] a similarity that we will discuss in more detail in a following section. However, we remark that in the case of a substrate such as **6*E*** this selectivity has no practical consequences since **2A**‡-**6*E*-*si*** and **2A**‡-**6*E*-*re*** lead to the same achiral product (see Chart 2).

Concluding this section, it is worthy to note a geometric feature of the forming five-membered ring. The CH_2 group close to the C═C double bond presents the two H atoms in an equatorial and an axial position. These H atoms are marked as pro-*R* and pro-*S* in Figure 3, according to the configuration (*R* or *S*, respectively) that would be assumed by the C atom to which they are bonded when they are replaced with a methyl group. This configuration would also correspond to the configuration of the products at the end of the metathesis reaction. In the case of **2A**‡-**6*E*-*si***, the pro-*R* H atom is in the axial position, and thus, it is labeled pro-R_{ax}, while the pro-*S* H atom is labeled pro-S_{eq} because it is in an equatorial position. A similar nomenclature is adopted for **2A**‡-**6*E*-*re***.

Relationship between Olefin Enantioface and Configuration of the Products. In this section we report on the enantioselectivity in the ring-closing metathesis of the chiral substrate **7*E*** of Chart 2. The conclusions for **7*E*** can easily be extrapolated to the experimental enantioselectivity observed in the desymmetrization of **5*E*** if the CH_3 group on the chiral C atom of **7*E*** is replaced with the $-C(CH_3)=CH(CH_3)$ group. As starting geometries we used **2A**‡-**6*E*-*si*** and **2A**‡-**6*E*-*re***, and we simply replaced one of the pro-*R* and pro-*S* H atoms with a methyl group.

First, we positioned the additional methyl group in the equatorial position, thus obtaining the **2A**‡-**7*E*-*si*-*S*$_{eq}$** and **2A**‡-**7*E*-*re*-*R*$_{eq}$** geometries. These transition states are illustrated in Figure 4, and are very similar to the corresponding transition states obtained for **6*E*** (compare Figures 3 and 4). In both transition states the additional group in the pseudoequatorial position is oriented in an empty area, substantially away from all the other groups of the system. From an energetic viewpoint, **2A**‡-**7*E*-*si*-*S*$_{eq}$** is more stable than **2A**‡-**7*E*-*re*-*R*$_{eq}$** by 10 kJ/mol. This energy difference is slightly higher than that between **2A**‡-**6*E*-*si*** and **2A**‡-**6*E*-*re***, 6 kJ/mol. These findings indicate that an additional substituent in the pseudoequatorial position is more easily positioned in **2A**‡-**6*E*-*si*** than in **2A**‡-**6*E*-*re***. This is reasonable, considering that the small geometric rearrangements needed to accommodate the additional group are not a problem in the relaxed **2A**‡-**6*E*-*si*** geometry. Instead, these rearrangements are slightly more difficult when the additional group in the pseudoequatorial position is added to the slightly compressed **2A**‡-**6*E*-*re*** geometry. The main point, however, is that formation of the (*S*)-product is favored when the additional group is inserted in the pseudoequatorial positions of **2A**‡-**6*E*-*si*** and **2A**‡-**6*E*-*re***.

The other competing transition state that would lead to an (*R*)-product, **2A**‡-**7*E*-*si*-*R*$_{ax}$**, has no relevance since it is 28 kJ/mol higher in energy than the most favored transition state, **2A**‡-**7*E*-*si*-*S*$_{eq}$**. In **2A**‡-**7*E*-*si*-*R*$_{ax}$** the additional CH_3 group is positioned in an axial position, and it is at short distances from the tail CH group of the reacting C═C double bond, and from the nearby iodine atom. Thus, in agreement with the experimental results, for an (*R*,*R*)-catalyst, formation of the (*S*)-enantiomer is favored over formation of the (*R*)-enantiomer, since **2A**‡-**7*E*-*si*-*S*$_{eq}$** is favored over both **2A**‡-**7*E*-*re*-*R*$_{eq}$** and **2A**‡-**7*E*-*si*-*R*$_{ax}$**. Finally, to test the influence of solvent effects on the energy differences, we calculated the relative stability of **2A**‡-**7*E*-*si*-*S*$_{eq}$**, **2A**‡-**7*E*-*re*-*R*$_{eq}$**, and **2A**‡-**7*E*-*si*-*R*$_{ax}$** in tetrahydrofuran, the solvent used experimentally. These calculations were performed with the COSMO implementation of ADF, and are reported in Table 1. Examination of the values indicates that solvent effects have a very small influence on the energy differences, and thus, the overall chemical picture we obtain remains confirmed. This result is in agreement with the experimental finding that solvent (THF, dichloromethane, benzene) has no significant effect on the enantioselectivity of these systems.[33] On the other hand, this conclusion is reasonable, since the competing diastereoisomeric transition states are structurally extremely similar.

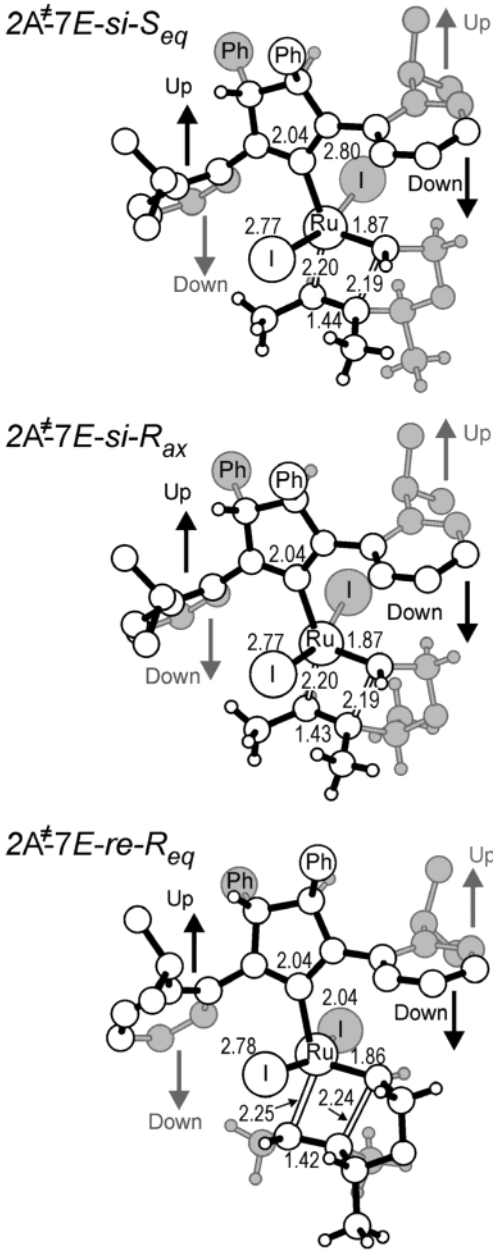

Figure 4. Transition states **2A**‡-**7*E*-*si*-*S*$_{eq}$**, **2A**‡-**7*E*-*re*-*R*$_{eq}$**, and **2A**‡-**7*E*-*si*-*R*$_{ax}$**, corresponding to ring-closing metathesis of **7*E*** with the catalyst derived from **2**. Distances are in angstroms.

(65) Corradini, P.; Guerra, G.; Cavallo, L. *Acc. Chem. Res.* **2004**, *37*, 231.
(66) Guerra, G.; Cavallo, L.; Corradini, P. *Top. Stereochem.* **2003**, *24*, 1.

Scheme 4

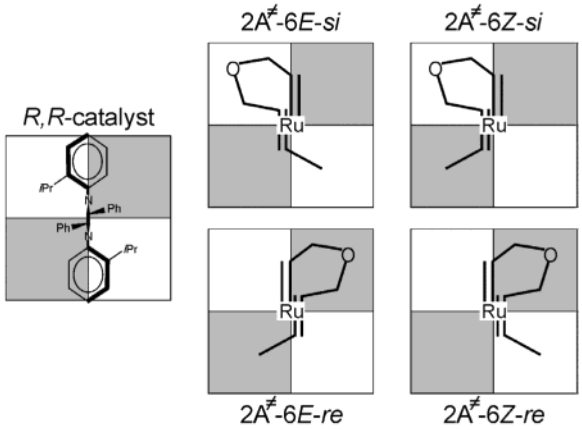

In conclusion, our analysis indicates that the chiral folding of the catalyst imposes a chiral orientation to the angle θ. This chiral orientation selects between the two enantiofaces of the olefin, and the more reactive transition state is characterized by having the additional R groups in a pseudoequatorial position of the forming five-membered ring.

This implies that, for an (*R*,*R*)-catalyst, values of $\theta \approx -90°$ and, consequently, ring-closing metathesis of the *si* enantioface is favored. In turn, the higher reactivity of the *si* enantioface implies that additional R groups in the equatorial pro-*S* position are favored. This flow of information rationalizes the obtainment of the (*S*)-enantiomer as a major product in the ring-closing metathesis of the achiral substrates **5*E*** with an (*R*,*R*)-catalyst.[33]

Role of the Halogens. In this last section we briefly discuss the role of the nature of the halogen atoms on the enantioselective performance of **2**. Experimentally, the heavier the halogen the greater the ee which is obtained in the desymmetrization of achiral substrates such as **5**. To this end we optimized the geometry of the (pre)catalysts as **2** of Chart 1, in which the carbene group =CHR is simply $=CH_2$, and PR_3 is the simple PH_3 phosphine. These optimizations were performed with Cl, Br, and I as halogens. The main geometric parameters that characterize the three structures, the folding angles ϕ_1 and ϕ_2 in particular, are very similar to each other. The only significant difference is in the X−Ru−X angle, which grows from 163° for Cl to 168° for Br to 176° for I. Smaller values of the X−Ru−X angle correspond to having the halogen atoms pulled away from the carbene moiety toward the empty coordination position *trans* to the Ru=C(carbene) bond. This finding suggests that, for the heavier halogens, the larger X−Ru−X angle associated with the larger van der Waals radius synergically creates a smaller reactive pocket for the ring-closing metathesis, enhancing the steric pressure of the chirally folded NHC ligand. Instead, with smaller X−Ru−X angles and with smaller halogens, the transition state corresponding to the wrong enantioface of the substrate can be accommodated better in a slightly larger reactive pocket.

Discussion and Outlook

Mechanism Validation. To provide a more general mechanism, we rediscuss the results using a representative sketch. Scheme 4 displays a quadrant representation of the transition states for ring-closing metathesis in the case of an (*R*,*R*)-catalyst.

The systems are viewed along the NHC−Ru bond, and the quadrants represent space occupation in the equatorial plane of the system. Gray quadrants correspond to zones sterically encumbered by the bent-down side of the N-bonded aromatic rings, while white quadrants correspond to less crowded zones, where the bent-up sides of the rings are positioned. Only the backbone of the substrate is represented. The favored **2A‡-6*E*-*si*** transition state presents both the terminal CH_3 group of the substrate and the CH_2O groups of the forming ring in open quadrants, whereas the less favored **2A‡-6*E*-*re*** transition state presents both in crowded quadrants. These transition states are illustrated in Figure 3.

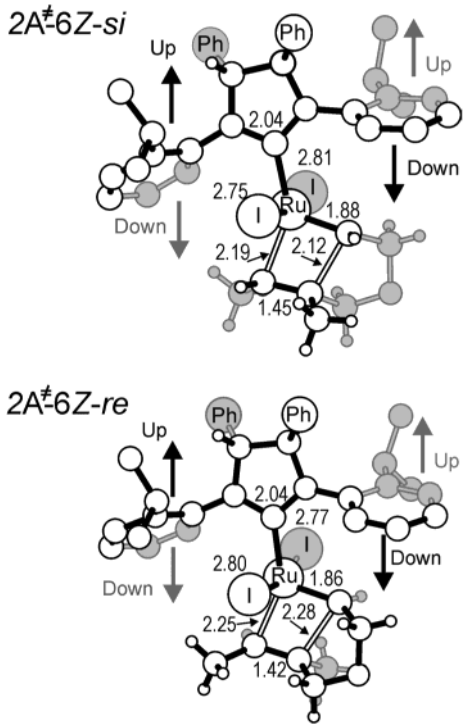

Figure 5. Transition states **2A‡-6*Z*-*si*** and **2A‡-6*Z*-*re***, corresponding to the ring-closing metathesis of **6*Z*** with the catalyst derived from **2**. Distances are in angstroms.

Instead, for a (*Z*)-substrate such as **6*Z***, both the **2A‡-6*Z*-*si*** and **2A‡-6*Z*-*re*** transition states present one of these groups in a crowded quadrant while the other is in an open quadrant. For **6*Z*** we calculated **2A‡-6*Z*-*si*** to be only 2 kJ/mol lower in energy than **2A‡-6*Z*-*re***, in agreement with the low experimental ee observed for (*Z*)-substrates. These transition states are illustrated in Figure 5.

On the other hand, chiral systems which cannot fold are also unable to transfer the information from the points of chirality to the substrate effectively. According to our calculations this occurs in the case of the catalyst derived from **3**. For substrate **6*E*** and a catalyst derived from **3** we calculated **3A‡-6*E*-*re*** to be only 3 kJ/mol lower in energy than **3A‡-7*E*-*si***, in agreement with the low ee experimentally observed. We correlate the low enantioselectivity of **3** to the small deviation from −90° of the angles ϕ_1 and ϕ_2 (see Figure 6 and Table 1), which corresponds to reduced chiral folding of the catalyst. Steric interactions between the Me groups on the N-bonded aromatic rings and the halide atoms bonded to the Ru atom hinder rotations around ϕ_1 and ϕ_2, constraining these angles close to 90°. This validates the mechanism we proposed.

Outlook. Our analysis suggests that more effective catalysts should present higher steric differences between gray and white quadrants. This could be accomplished either by catalysts that

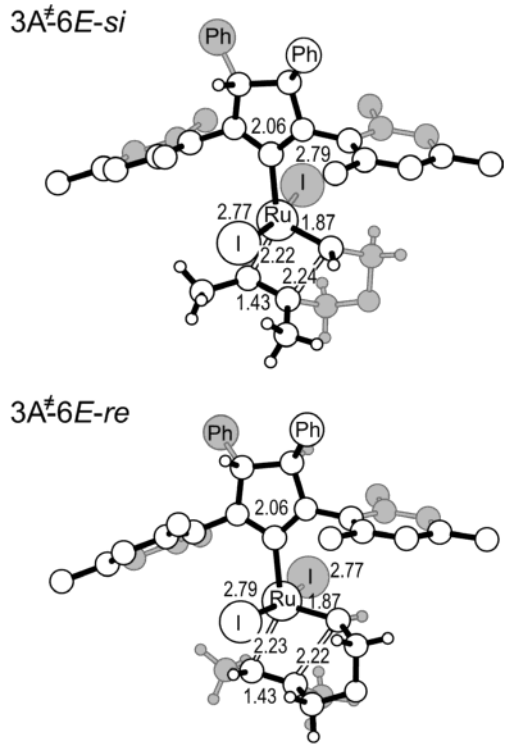

Figure 6. Transition states **3A‡-6*E*-*si*** and **3A‡-6*E*-*re***, corresponding to the ring-closing metathesis of **6*E*** with the catalyst derived from **3**. Distances are in angstroms.

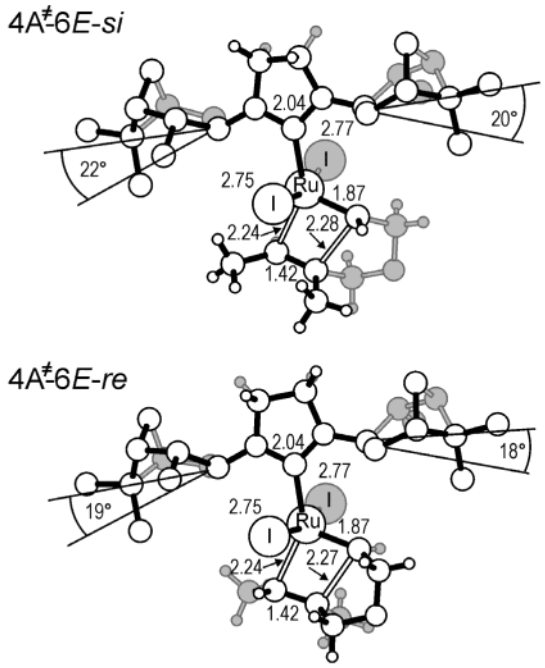

Figure 7. Transition states **4A‡-6*E*-*si*** and **4A‡-6*E*-*re***, corresponding to the ring-closing metathesis of **6*E*** with the catalyst derived from **4**. Distances are in angstroms.

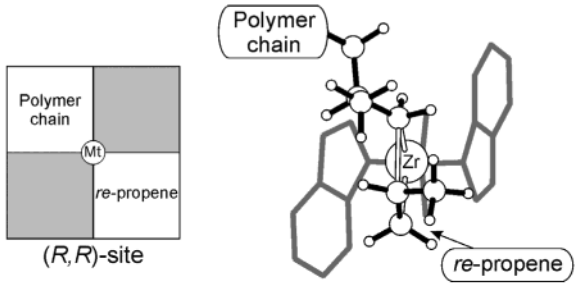

Figure 8. Favored transition state for the propagation step in the propene polymerization with a bis(indenyl)-based zirconocene, on the right. Quadrant representation of the same transition state, left. Gray quadrants correspond to zones sterically encumbered by the six-membered rings of the bis(indenyl) ligand, while white quadrants correspond to less crowded zones.

result in more pronounced bent-up and bent-down sides of the N-bonded aromatic ring or, alternatively, by ligands with chiral N-bonded groups that would locate bulky groups in the gray quadrants. The catalysts proposed by Hoveyda[34] can be considered as a special case of this second class. In contrast, the diisopinocampheol-based catalyst tested by Grubbs[33] is an attempt in the right direction, but the chiral information on the catalyst is not transferred effectively to the substrate.

According to our calculations, for the model of a catalyst based on **4**, transition state **4A‡-7*E*-*si*** is only 1 kJ/mol lower in energy than **4A‡-7*E*-*re***, in agreement with the low ee experimentally observed. We associate the low enantioselectivity of **4** to the sp^3 hybridization of the C atoms of the isopinocampheol groups bonded to the N atoms of the NHC ring (see Figure 7), which bend the whole chiral isopinocampheol group away from the substrate by roughly 20°. This results in long distances between the chiral atoms of the isopinocampheol group and the substrate and, consequently, in a poor transfer of asymmetric information. On the contrary, in the effective system **2**, the sp^2 hybridization of the C atoms at the junction of the aromatic groups with the NHC ring bend the N-boned aromatic rings toward the plane defined by the Ru and halide atoms. This results in an effective transfer of asymmetric information between the bent-down side of the N-bonded aromatic groups and the substrate.

In short, our calculations indicate that the origin of enantioselectivity with these catalysts is connected to the chiral folding of the N-bonded aromatic rings which is imposed by the Ph groups in positions 4 and 5 of the NHC ring. Within this mechanism, there are no direct interactions between the chiral points of the catalyst and the substrate. Instead, the N-bonded aromatic rings act as messengers between the points of chirality and the substrate, forcing a chiral orientation around the angle θ. This chiral orientation around the Ru=C bond finally selects between the two enantiofaces of the olefin.

This mechanism of selectivity can be tightly correlated to the mechanism of stereospecificity in the polymerizations of propene with group 4 catalysts.[36,65,66] In fact, also in this case there is a messenger between the points of chirality and the substrate. The messenger is the chiral orientation of the growing polymeric chain, and this situation is illustrated in Figure 8 for the prototype isospecific zirconocene containing the bis(1-indenyl) ligand.

In the case of an (*R*,*R*)-metallocene, the most stable transition state for primary propene insertion into the Zr−isobutyl bond (which simulates a primary growing chain) corresponds to the insertion of an *re*-propene molecule, and it shows the most classical features which characterize the mechanism of the chiral orientation of the growing chain. These are (i) the growing chain assumes a chiral orientation to minimize steric interactions with the chiral ligand and (ii) the monomer inserts with the methyl group *trans* oriented relative to the growing chain, to minimize its steric interaction with the growing chain itself.

This situation is schematically sketched in the quadrant representation of Figure 8. The lowest energy transition state places both the chain and the propene methyl group in an open quadrant. The overall similar space occupation between the structure of Figure 8 and that of **2A**‡**-6*E*-*si*-S_{eq}**, and the same quadrant representation, supports a unified view of the mechanisms of stereoselectivity with these very different catalysts.

Conclusions

We investigated the origin of enantioselectivity in the asymmetric olefin metathesis with the NHC-based Ru catalysts. The main conclusions of our work can be summarized as follows.

(i) The most classical intermediate **A** of Scheme 2, with the substrate coordinated *trans* to the NHC ligand, is the key intermediate also in asymmetric metathesis reactions. Alternative intermediates such as **B** and **C**, with the substrate coordinated *cis* to the NHC ligand, are of remarkably higher energy. This conclusion is in agreement with other studies on closely related systems.

(ii) In the most stable coordination intermediate **A** the angle θ assumes a value close to 180°, to reduce steric interactions between the R group bonded to the carbene C atom and the N-bonded aromatic rings. In the four-center transition state for metallacycle formation, θ assumes values close to |90°|. Values of $\theta \approx -90°$ and $+90°$ imply coordination and reaction of the *si* and *re* enantiofaces of the double bond, respectively. In both transition states these combinations ($\theta \approx -90°$/*si* enantioface and $\theta \approx +90°$/*re* enantioface) place the forming five-membered rings on one side of the forming metallacycle ring. This reduces steric interactions with other atoms and allows the forming five-membered ring to assume a relaxed pseudoenvelope geometry.

(iii) The two Ph groups in positions 4 and 5 of the imidazolyl ring of the NHC ligand impose a chiral folding to N-bonded aromatic groups. In particular, the side of the N-bonded aromatic group near the Ph group is bent down, that is, bent toward the Ru atom and the substrate. Obviously, the other side of the N-bonded aromatic group is bent away. This structural feature is found in all the geometries we calculated, and is also found in the crystal structure of the (pre)catalyst.

(iv) The folding of the catalyst implies a chiral orientation of the dihedral angle θ in the transition state. The preferred orientation is the one that places the R group bonded to the Ru═C carbene atom away from the bent-down side of the N-bonded aromatic group. For an (*R*,*R*)-configuration of the catalyst, this implies that values of $\theta \approx -90°$ are favored. On the basis of point ii above, it is implied that with an (*R*,*R*)-catalyst the *si* enantioface of the substrate is more reactive.

(v) An additional R group near the reacting C═C double bond of the substrate is rather easily accommodated in a pseudoequatorial position, independently of the reacting enantioface of the substrate. Conversely, transition states with the additional group in a pseudoaxial position are of remarkably higher energies.

Scheme 5

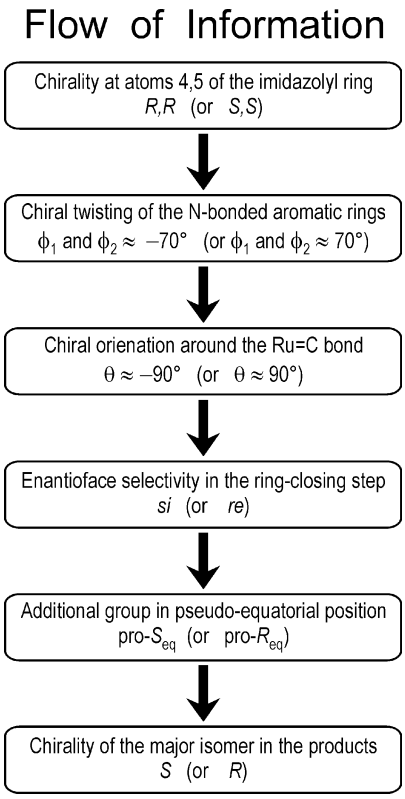

The flow of information from the points of chirality to the preferential configuration of the products is displayed in Scheme 5. The chiral orientation of the dihedral angle θ around the Ru═C bond acts as a messenger of information between the chiral folding of the ligand and the reacting enantioface of the substrate.

The main aim of the present work was to rationalize the origin of selectivity in the asymmetric Ru-catalyzed ring-closing metathesis reactions at the molecular level. We believe that our study rationalizes the origin of enantioselectivity experimentally reported for the desymmetrization of achiral trienes. We also believe that our detailed rationalization can contribute to the rational design of new catalysts with better performance, or to new applications of already discovered catalysts.

Acknowledgment. We thank Dr. H. Jacobsen, KemKom Canada, for critical discussion. This work was supported by the MURST of Italy (Grants PRIN 2002 and FISR) and by Basell Polyolefins. We thank Prof. Tom K. Woo and the SHARCNET Project, University of Western Ontario, for generous access to computer resources.

Supporting Information Available: Cartesian coordinates of all the structures reported in the paper. This material is available free of charge via the Internet at http://pubs.acs.org.

JA0484303